Hindawi
Journal of Sensors
Volume 2023, Article ID 9782134, 1 page
https://doi.org/10.1155/2023/9782134

Retraction

Retracted: Luminosity Control and Contrast Enhancement of Digital Mammograms Using Combined Application of Adaptive Gamma Correction and DWT-SVD

Journal of Sensors

Received 19 December 2023; Accepted 19 December 2023; Published 20 December 2023

This article has been retracted by Hindawi following an investigation undertaken by the publisher [1]. This investigation has uncovered evidence of one or more of the following indicators of systematic manipulation of the publication process:

(1) Discrepancies in scope
(2) Discrepancies in the description of the research reported
(3) Discrepancies between the availability of data and the research described
(4) Inappropriate citations
(5) Incoherent, meaningless and/or irrelevant content included in the article
(6) Manipulated or compromised peer review

The presence of these indicators undermines our confidence in the integrity of the article's content and we cannot, therefore, vouch for its reliability. Please note that this notice is intended solely to alert readers that the content of this article is unreliable. We have not investigated whether authors were aware of or involved in the systematic manipulation of the publication process.

Wiley and Hindawi regrets that the usual quality checks did not identify these issues before publication and have since put additional measures in place to safeguard research integrity.

We wish to credit our own Research Integrity and Research Publishing teams and anonymous and named external researchers and research integrity experts for contributing to this investigation.

The corresponding author, as the representative of all authors, has been given the opportunity to register their agreement or disagreement to this retraction. We have kept a record of any response received.

References

[1] D. Kumar, A. K. Solanki, and A. K. Ahlawat, "Luminosity Control and Contrast Enhancement of Digital Mammograms Using Combined Application of Adaptive Gamma Correction and DWT-SVD," *Journal of Sensors*, vol. 2022, Article ID 4433197, 18 pages, 2022.

Hindawi
Journal of Sensors
Volume 2022, Article ID 4433197, 18 pages
https://doi.org/10.1155/2022/4433197

Research Article

Luminosity Control and Contrast Enhancement of Digital Mammograms Using Combined Application of Adaptive Gamma Correction and DWT-SVD

Dharmendra Kumar,[1] **Anil Kumar Solanki**,[2] **and Anil Kumar Ahlawat**[3]

[1]*Ajay Kumar Garg Engineering College, Ghaziabad, Affiliated to Dr. APJ Abdul Kalam Technical University, Lucknow, India*
[2]*Bundelkhand Institute of Engineering and Technology, Jhansi, India*
[3]*KIET Group of Institutions, Ghaziabad, Affiliated to Dr. APJ Abdul Kalam Technical University, Lucknow, India*

Correspondence should be addressed to Dharmendra Kumar; malik.dharam@gmail.com

Received 9 March 2022; Revised 1 May 2022; Accepted 16 May 2022; Published 1 June 2022

Academic Editor: Sheng Du

Enhancement of mammogram images against low-contrast and poor illumination is still a challenge for researchers. Focusing on such issues, this manuscript presents a two-stage enhancement technique for mammogram images. The first stage of the image enhancement deals with illumination control using the corrective-adaptive gamma correction (CAGC) approach. In the second stage, contrast enhancement operation on the luminosity-controlled image is incorporated. In order to enhance visual perception against low-contrast, the combined application of discrete wavelet transform (DWT) and singular value decomposition (SVD) is incorporated. The experimentation of the proposed technique was performed over a publicly available mini-MIAS dataset. The proposed technique is evaluated on various quantitative parameters such as Pearson correlation coefficient (PCC), universal image quality index (IQI), structural similarity index measurement (SSIM), contrast improvement index (CII), average mean brightness error (AMBE), and mean absolute error (MAE) and obtain the average values of 0.996, 0.912, 0.921, 1.098, 15.732, and 15.624 that are promising results as compared to the other traditional methods. This study also compares the proposed technique with state-of-art methods and achieves better performance, resulting in significant improvement in contrast enhancement and local information preservation of mammogram images.

1. Introduction

Breast cancer is one of the most common diseases among women aged between 35 and 55 years. According to the National Cancer Institute (NCI), one out of every eight women in the United States is suffering from breast cancer during their lifetime [1]. However, in breast cancer treatment, the foremost step is to detect it in the early stage, and an effective method is required to reduce its mortality. This leads to a need for breast examination that can be done by several techniques, namely, magnetic resonance imaging (MRI), optical tomography/spectroscopy (OT/S), X-ray imaging (X-ray) imaging, positron emission tomography (PET) imaging, ultrasound imaging (UI), and computerized tomography (CT) imaging. Among these techniques, mammography (X-ray image) is the oldest and popular technique in which low-energy X-rays are used to create images of the woman's breast. These X-ray images are used by radiologists to detect and diagnose cancer [2, 3]. In radiological practice, mammography is of two types: film mammography and digital mammography. The radiologist mainly uses digital mammography because of its better-quality imaging and requirement of a lower X-ray dose.

In standard mammography, the tumors are not adequately visible due to low luminosity and poor contrast that may hurdle in the early diagnosis of diseases. The luminosity of mammogram images is degraded because of the uneven illumination produced by the imaging devices and low lighting conditions, which further obscures the detection of small details and visual perception during a mammogram

screening [4, 5]. The enhancement of mammograms is a crucial part of medical imaging that can be done by removing the noise and doing contrast enhancement that helps to detect the essential features in mammograms. To improve the visual quality of mammograms, this work provides two stages in a pipeline design, combining luminosity management in the first stage and afterward passing it to the contrast enhancement stage. The first stage uses the CAGC method to improve the visual appearance and control luminosity by dynamically calculating the intensity transformation function based on mammography statistical parameters. In the second stage, the contrast enhancement is performed using DWT and SVD operations over the image processed in the first stage; it further enhances the mammogram image by preserving local information. In general, DWT is used to convert the image from spatial domain to frequency domain, and four frequency subbands are obtained, namely, LL, LH, HL, and HH [6]. In order to protect edge information, only the LL subband is considered for contrast enhancement. The SVD is a technique used to compute a singular value matrix by factorizing a matrix into three matrices [7]. Singular value matrix includes intensities information when applied on LL subbands and used for image equalization. The references are made to the detailed study of DWT and SVD [8, 9]. The proposed method has been tested on the mini-MIAS database [10].

The remaining paper is organized in the following sections, as Section 2 includes state-of-the-art methods in the concerned field. Section 3 presents the proposed method comprises a detailed description of the luminosity control and contrast enhancement procedures. Experimental results and discussions are presented in Section 4, and the conclusion part of this paper is presented in Section 5.

2. Literature Review

Lots of work have been done in the past on the enhancement of mammograms. Patrick et al. [11] used a density-weighted contrast enhancement (DWCE) as an enhancement technique for mammograms. The key idea behind this algorithm is that it uses each pixel's local density value to weight its local contrast by reducing the background and noise while retaining the valuable information of original mammograms. Pisano et al. [12] proposed the contrast limited adaptive histogram equalization (CLAHE), which works by calculating the histogram for contextual region information of the image. The contrast enhancement factor is the primary target of CLAHE. It reduces the edge-shadowing effect and prevents the image from overenhancing noise, which is the disadvantage of adaptive histogram equalization (AHE). The size of pixels in the histogram's contextual region and clip level is used as a parameter of CLAHE. However, this method fails in enhancing fatty areas as CLAHE degrades performances in fatty areas. Jin et al. [13] proposed a multiscale expansion of AHE in which different filters such as low-pass and high-pass filters are used. When multiscale adaptive histogram equalization (MAHE) was compared with CLAHE, it was observed that the CLAHE had enlarged the nodule of the chest image while the MAHE enhanced the nodule appearance without changing its size. Thus, this algorithm enhances the image and also shows fine interstitial markings in the lung's periphery. Wu et al. [14] introduced an improved high-pass filter by combining it with the unsharp masking (UM). The sharpening effect at a low enhancement factor can be enhanced by using a better high-pass filter. Recently, Sundaram et al. [15] proposed a histogram-modified CLAHE (HM-CLAHE) to adjust the level of the contrast enhancement, and parameter-like enhancement measure (EME) is determined for performance evaluation as CLAHE was not alone successful in preserving the local details of the mammograms. Later, Sundaram et al. [16] introduced HM-LCE for mammogram images. This approach greatly improves the local details of the resulting image by using a modification function to change the histogram of the original image. However, it fails to capture hidden details of the image adequately. Panetta et al. [17] proposed a naïve approach for mammogram enhancement that uses nonlinear unsharp masking (NLUM). The benefit of this approach is that no prior knowledge of the image content is required.

Huang et al. [18] suggested a hybrid histogram-based approach using transform-based gamma correction (TGC) and traditional histogram equalization (THE). This approach was inspired by the technique proposed in [19] as its cumulative distribution function (CDF) is applied as a normalized gamma function to modify the transformation curve without losing histogram statistics. The weighted distribution (WD) function applies to modify the histogram with the original image smoothed by weighted distribution. Later, Kaur and Singh [20] proposed a method to divide the image into histograms up to some recursive level. In order to perform segmentation, this study applied two segmentation methods, namely mean sub-histogram segmentation and median sub-histogram segmentation. Then, the WD function is applied along with the gamma correction, giving an overall enhanced image. Anand and Gayathri [21] introduced a two-step adaptive histogram equalization; the first step of AHE was followed by another step of AHE. Applying another conventional AHE is used to present more hidden internal features because of more contrast information. Recently, Jenifer et al. [22] presented a fuzzy clipped contrast limited adaptive histogram equalization (FC-CLAHE) system based on a fuzzy rule-based clip limit that selects the clip limit automatically based on mammogram characteristics. This technique provides sufficient contrast enhancement.

Most of the prevailing techniques for enhancing mammograms mainly focus on the brightness and contrast enhancement of the images. The major disadvantage of these approaches is that after histogram equalization, the brightness of an image can be modified. It is all because of the faltering characteristic of histogram equalization. This partitioning method uses the mean threshold value for the partition of the histogram's gray levels. After the partition into subimages, one of the subimages is equalized up to the mean, while the other subimage is equalized over the range of the mean depending on the respective histogram. Kim [23] suggested a brightness preserving bihistogram equalization (BBHE) approach for preserving mean brightness while

increasing contrast. Wang et al. [24] proposed a technique known as dualistic subimage histogram equalization (DSIHE) to partition the histogram's gray level using median threshold value instead of mean value threshold taken in BBHE. DSIHE was proposed in order to overcome the change in the luminosity of the image after HE. DSIHE gives better equalizing results by keeping the original image luminance well enough and contrasting the low-intensity pixel value. Huang et al. [18] suggested an adaptive gamma correction (AGC) method for image enhancement that uses weighing distribution. This method uses a CDF and a normalized gamma function to change the transformation curve without affecting the available histogram. Then, further weighting distribution is also applied to lessen the generation of adverse effects used to smooth the fluctuant phenomenon, and final gamma correction is applied over the CDF as an adjustment parameter. Later, a fuzzy-based BBHE method was proposed by Sheba and Gladston Raj [25] to overcome the luminance and brightness's uncontrollable change. Fuzzy-based BBHE is a three-step procedure. In the first step, gray-level intensities are converted into an adaptive fuzzy plane with a scale of 0 to 1. In the second step, BBHE is applied to the fuzzy domain, and the fuzzy plane is mapped back to the gray level image in the final step. Chen and Ramli [26] proposed recursive mean separate histogram equalization (RMSHE), which partitions the histogram of a given image recursively. Each segment is equalized independently, and the contrast-enhanced output is obtained by adding all of the segments together. The drawbacks of RMSHE are its large time complexity due to the recursion process.

In another approach, Demirel et al. [27] introduced DWT-SVD technique to enhance the satellite image. This method applies the SVD to the input image and the enhanced image processed with GHE. The SVD method is applied on low-frequency LL subband obtained using DWT. The new LL subband is obtained by multiplying the correction coefficient by the singular value matrix. Inverse DWT is used to obtain the equalized satellite image. This method produces a higher contrast and clearer enhanced image. Further, Kallel and Ben Hamida [28] suggested the use of AGC with DWT-SVD in series to enhance noncontrast CT images. The gamma correction is determined dynamically based on statistical information of the image in this approach. Zhou et al. [29] suggested a method where the image was enhanced by controlling its luminosity by splitting up its hue, saturation, and value color bands and focusing on the value color band. A luminance gain matrix is computed using the gamma correction function on the luminosity channel. Finally, the resultant image is formed by enhancing the contrast using the CLAHE method in color retinal images. Gupta and Tiwari [30] proposed an enhancement technique for luminosity enhancement based on adaptive gamma correction and quantile-based contrast enhancement with the application on color retinal images. In another work by Palanisamy et al. [31] introduced an improved enhancement framework for color fundus images where gamma correction and SVD are used for luminosity enhancement on the value channel. Then, the contrast of the resultant image is improved using CLAHE. Recently, Pawar and Talbar [32] introduced an approach based on the fusion of DWT coefficients of the original image and CLAHE enhanced image, considering the maximum entropy value. In this method, three levels of decomposition of images are done using Haar wavelet. At each level, the approximate coefficient is fused with the averaging operation, while the detailed coefficient is fused by calculating the entropy of the image considering the maximum entropy value. This method provides sufficient contrast enhancement. Gandhamal et al. [33] proposed a generalized contrast enhancement approach for medical images. This method used the gray level S-curve transformation technique, which increases the difference between the minimum and maximum gray values, leading to strengthening edges between adjacent tissues. This method is able to produce good contrast, but it suffers from blocking artifacts. In addition to this, for improving the contrast of mammogram images, El Malali et al. [34] produces a method that modified local S-Curve transformation based on a multiobjective genetic algorithm. Fuzzy weighted histogram equalization (FWHE) was proposed by Magudeeswaran and Balasubramanian [35], in which intensity fuzziness is adjusted by using contrast intensification operator, and weighting and thresholding are applied to modify the PDF of fuzzy matrix followed by HE procedure on the mammogram image. Siddiqi et al. [36] present a two-stage fuzzy blend scheme (FBS) on CT images of liver cancer. In the first stage, this technique uses a nonlinear filter for preprocessing of the image, and in the second stage, the fuzzy transformation function is used on the preprocessed image to produce a contrast-enhanced image.

From the preceding discussion, it is evident that the preservation of structural details is essential in the diagnosis of medical images. Due to blurring, uneven illumination created by imaging devices, patient position, and low lighting conditions, medical images suffer from complex noise and low contrast, further obscuring the identification of small details and visual perception during a medical image screening. As a result, it is essential to improve the luminance of the medical images before enhancing the contrast. In literature, various approaches for increasing luminosity have been proposed and out of which gamma correction is the popularly used method. However, with traditional gamma correction, the gamma value is selected manually, which does not provide adequate enhancement for all types of images [37]. To overcome this limitation, the proposed study uses CAGC that automatically sets the value of gamma according to the statistical characteristics of mammogram images. In order to improve the contrast of medical images, several methods are also discussed in the literature, but preserving edge details along with local contrast enhancement is still a challenge [29, 38, 39]. To deal with the aforementioned problem, this work proposes a combined application of DWT and SVD. The primary benefit of this technique is that it achieves sufficient contrast enhancement with maintaining the structural similarity in the original mammogram image without losing its clinical information content.

In summary, the key contribution of this study is as follows:

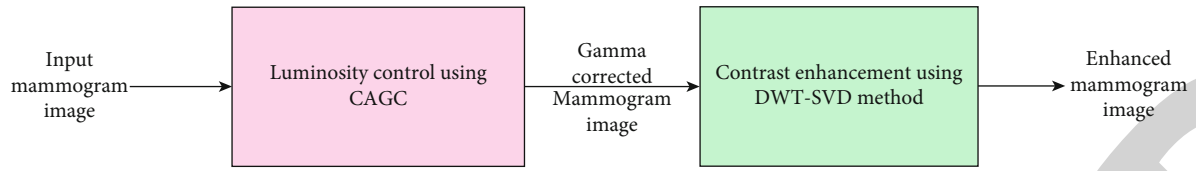

Figure 1: Block diagram of the proposed method.

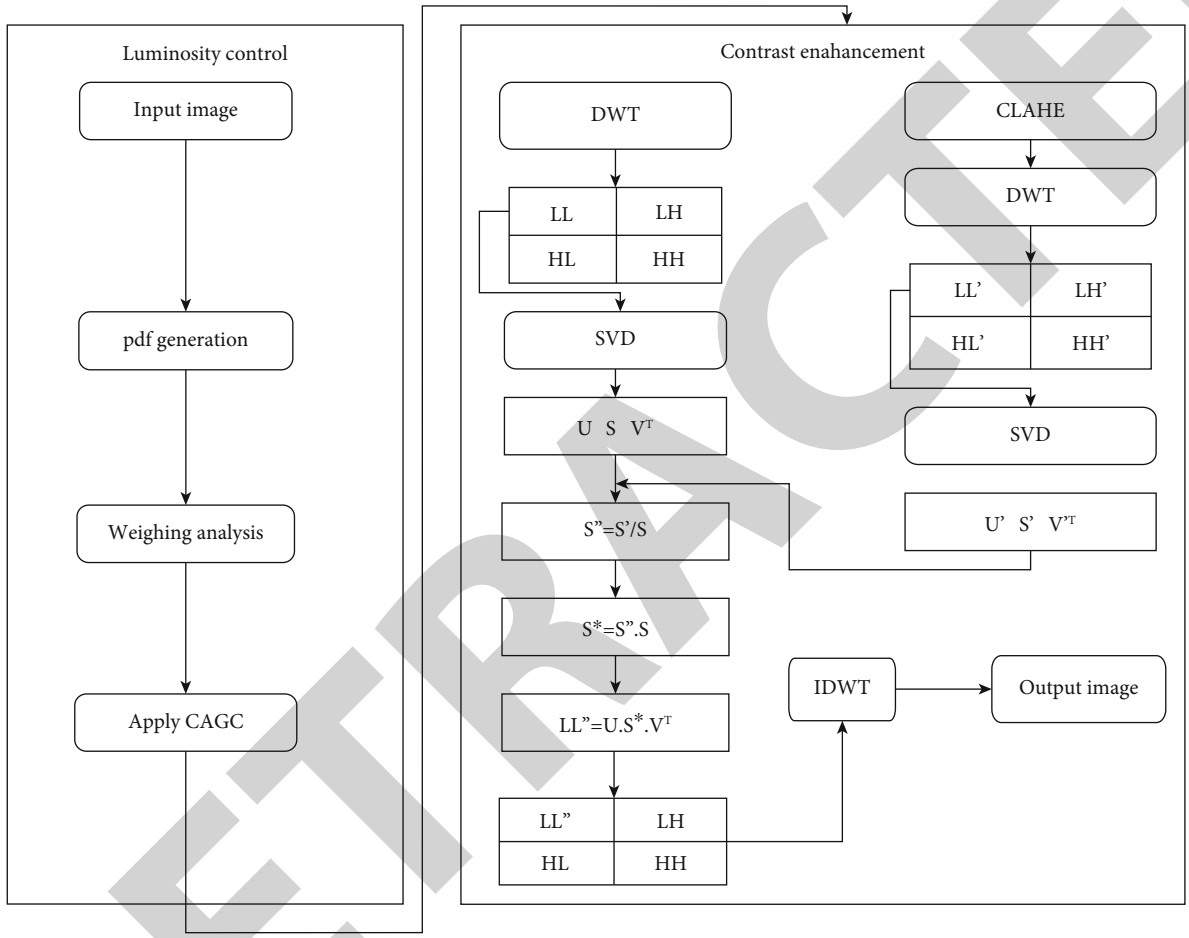

Figure 2: Detailed description of the proposed method.

(i) To improve the overall luminance of the mammogram images, proposed architecture utilizes CAGC procedure, an improved version of gamma correction method

(ii) To improve the local contrast and preserving edge details, a two-way DWT and SVD approach is incorporated to get corrective adjustment coefficient

(iii) The comparative analysis of the proposed method based on various quantitative parameters with traditional and state-of-art methods is presented

3. Proposed Method

Focusing minimization of interpixel error between original and enhanced image and maintaining the structural similarity between them, this section proposes a two-stage methodology for image enhancement. In the first stage, the luminosity of the mammograms is controlled by using the CAGC method. The second stage presents the contrast enhancement of the resulting mammogram from the previous stage. The block diagram and the detailed description of the proposed technique are illustrated in Figures 1 and 2. The detailed discussion of both approaches is given separately in the following subsections.

3.1. Luminosity Control. Luminosity refers to the object's perceived brightness by the human observer. The luminosity control will balance poor luminance image's overall luminosity. The mammogram images are suffered from poor luminosity due to the uneven illumination produced by the imaging devices and low lighting conditions, which

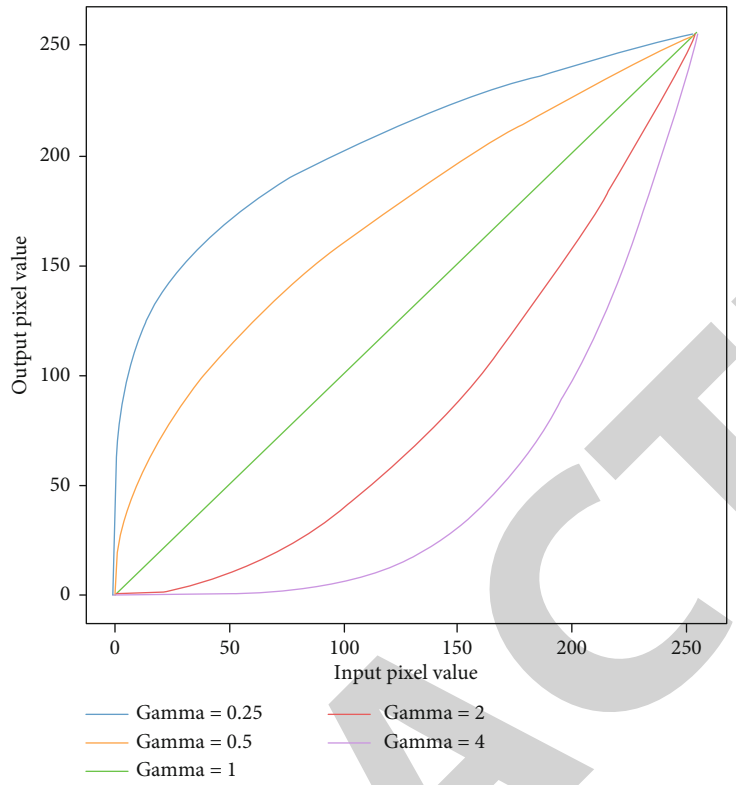

Figure 3: Transformation curve for different values of γ.

further obscures the detection of small details and visual perception during the screening of mammograms. Therefore, luminosity control is needed to be enhanced for better visual perception of mammogram images which helps in further diagnosis. There are various methods available in the literature for luminosity control of an image, out of which gamma correction is popularly used to enhance medical images. The mathematical expression for the gamma correction is as follows [28].

$$O = cI^{\gamma}, \tag{1}$$

where I and O are the intensities of input and output image. The c and γ are the parameters that control the sharpness of the transformation curve. Figure 2 illustrates the transformation curves for various values of γ.

Figure 3 shows that the dynamic range of lower pixels increases as $\gamma < 1$ while the dynamic range of higher pixels suppresses when $\gamma > 1$. In the case of $\gamma = 1$ reflects the identity; hence, the image luminosity does not change.

Adaptive gamma correction is a computationally efficient method to enhance the visual information of images [30]. Thus, adaptive gamma correction has been modified for mammogram images which dynamically calculate the intensity transformation function according to mammogram statistical characteristics and are referred to as the corrective-adaptive gamma correction method. The proposed CAGC

procedure CAGC
1. $w \longleftarrow CumSum(pdf_w)/Sum(pdf_w)$
2. max $Val \longleftarrow 2^8 - 1$
3. $l \longleftarrow 0$ to max Val
4. $i \longleftarrow 0$
5. ***while*** $i < 256$
6. $\quad l(i) = l_{\max}.(l(i)/\max Val)^{1-w(i)}$
7. $\quad i \longleftarrow i + 1$

Algorithm 1: Corrective adaptive gamma correction.

method is used to control the luminosity of the mammogram image as follows:

(1) Generate the probability distribution function (pdf) under the range of [0-255]

(2) Observe the maximum and minimum probability count in the image

(3) Calculate the weighing factor using the following equation

$$W(l) = \frac{\sum_{i=0}^{l} pdf_w(i)}{\sum_{i=0}^{\max Val} pdf_w(i)}. \tag{2}$$

(a) (b)

Figure 4: Original Image and enhanced image.

(4) Apply the CAGC procedure onto the original image based on the weighing factor calculated in step 3

3.2. Contrast Enhancement. In any subjective measurement of image quality, contrast is a significant factor in the luminance difference reflected from two adjacent surfaces. Poor contrast degrades the visual quality of an image. Therefore, to improve an image's visual quality, contrast enhancement is necessary, optimizing the contrast representing the critical information of an image. The intensity transformation function is given by

$$O = f(I), \tag{3}$$

where f is the transformation function used to map the intensity values I of the input image into intensity values O of the enhanced image. Various transformation functions can be used to enhance the contrast of an image [40]. Using histogram equalization, the example of contrast enhancement is shown in Figure 4.

The luminosity control can balance the overall luminance of low luminosity mammogram images, which leads to enhancing the image contrast up to some extent. However, a contrast enhancement technique is required to improve the local characteristics of mammogram images further. The following are the steps associated with the proposed contrast enhancement technique using combined DWT-SVD.

(1) Apply one-level DWT to the luminosity-controlled image as observed from the first stage and obtain the low-frequency sub-band "LL"

(2) Parallelly, apply the CLAHE approach to the image obtained from the first stage and observe the LL' subband of the modified image by applying the one-level DWT

(3) Singular value decomposition (SVD) operation is performed separately over the low-frequency subbands obtained from step 1 and step 2

$$\text{SVD}(LL) = U\,S\,V^T, \tag{4}$$

$$\text{SVD}\left(LL'\right) = U'S'V'^T. \tag{5}$$

(4) Calculate the corrective adjustment coefficient S''

$$S'' = \frac{\max\left(S'\right)}{\max\left(S\right)}. \tag{6}$$

(5) Obtain the modified singular matrix S^*

$$S^* = S.S.''. \tag{7}$$

(6) Applying inverse SVD operation using original values of U, V^T (obtained in eq. (4)) and S^*

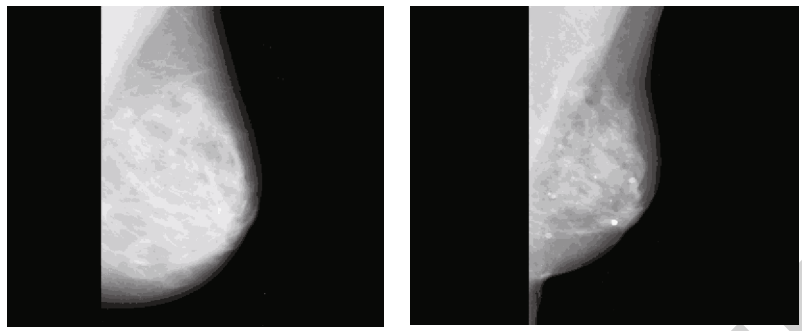

(a) I-1

(b) I-2

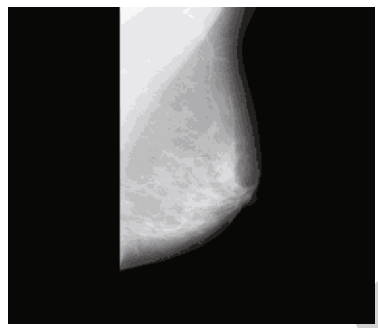

(c) I-3

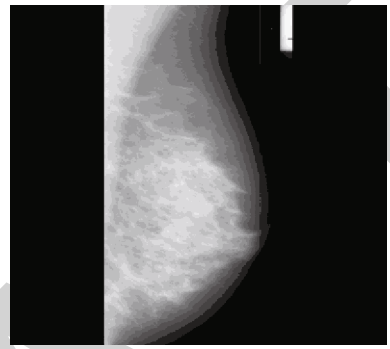

(d) I-4

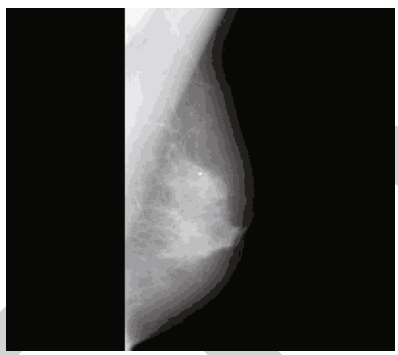

(e) I-5

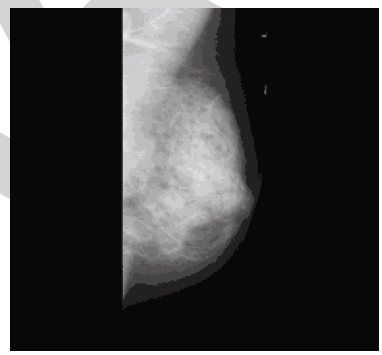

(f) I-6

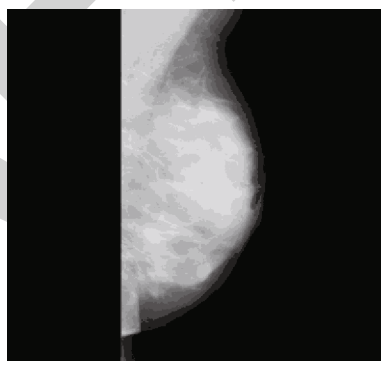

(g) I-7

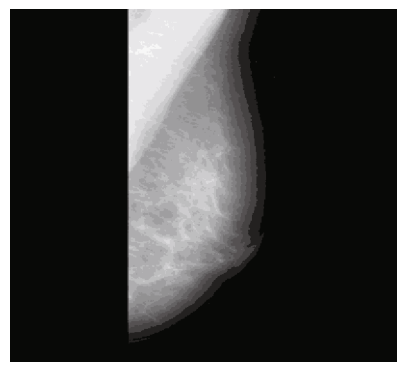

(h) I-8

Figure 5: Continued.

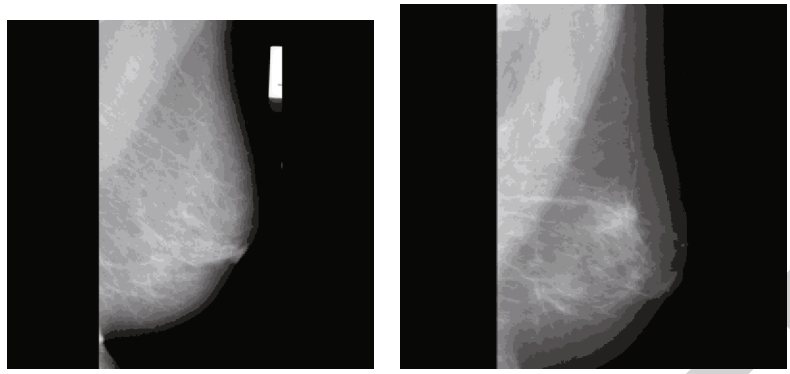

(i) I-9 (j) I-10

Figure 5: Original mammogram images (I-1 to I-10).

(calculated in eq. (7)), the enhanced subband of low-frequency component (LL'') is generated

(7) Perform inverse DWT operation over the modified subband LL'' and original subbands LH, HL, and HH to obtain the enhanced image.

After performing a two-stage enhancement operation (luminosity control and contrast enhancement), the obtained image is perceptually much better and very useful to medical practitioners to properly diagnose cancerous locations.

4. Experimental Results and Discussion

This section describes the experimental results of the proposed scheme and its comparative analysis with other traditional schemes such as HE, CLAHE, AGCWD, BBHE, and DSHIE. In order to demonstrate the suitability of the proposed scheme, we also compared its performance with other state-of-art methods. Due to uniformity, all the traditional and state-of-art methods are reimplemented on same architecture and same dataset. The proposed method optimally deals with the image enhancement errors while posing the required degree of enhancement. The performance of the proposed algorithm is tested over a large dataset of mammogram images (1024×1024) of mini-MIAS [10]. The mini-MIAS dataset contains 322 mammogram images that comprise 207 normal, 64 benign, and 51 malignant mammograms. However, for the sake of brevity, the results of ten sample images are presented, which comprise benign and malignant with different categories (fatty, fatty glandular, dense glandular, etc.) mammogram images. The hardware and software configurations for the proposed technique are used as Intel (R) Core (TM) i-3-4005 U CPU @ 1.70GHz, windows-10 (64-bit operating system), and MATLAB (R2019). The performance of the proposed method is shown by visual appearance and various quantitative metrics. We evaluate the result of enhanced mammogram images based on enhancement quality as well as on enhancement errors.

4.1. Qualitative Assessment. The objective of the enhancement of a mammogram is to identify the cancerous tissue present in the image. Several factors like uneven illumination and image acquisition restriction cause the low-contrast image, which may affect the diagnosis of mammograms. Hence, an effective contrast enhancement in a mammogram is required to present the resultant image visually apparent and to preserve the clinical information content. The proposed method's performance is evaluated based on visual assessment and quantitative assessment using image enhancement quality and image enhancement error measures. Figure 5 shows the low-contrast original mammogram images, and the corresponding histogram of the original images is given in Figure 6. Figures 7(a)–7(f) show the enhanced mammogram image corresponding to the input image I-1 after applying AGCWD, BBHE, CLAHE, HE, DSHIE, and the proposed methods, respectively. One can observe in Figure 7 that the proposed technique results are perceptually better and maintain the critical information in the enhanced image. Figure 7(a) illustrates that enhanced image using AGCWD suffers from overenhancement, leading to the misconception of information present in the mammogram image. In Figures 7(b)–7(c), the enhanced image produced by BBHE and CLAHE provides high contrast but suffers due to the introduced noise in the image. The enhanced image using DSHIE does not observe as perceptually good quality due to the lack of edge perseverance characteristic, shown in Figure 7(d). Figure 7(e) illustrates that the resulting image using HE is too bright due to the high AMBE value. Here, one can observe that the enhanced image through the proposed scheme given in Figure 7(f) is visually better with other traditional methods. It enhances the local features of mammograms while preserving the edge details. The histograms of enhanced images applying various methods, including the proposed one, are given in Figure 8.

4.2. Quantitative Assessment. This section depicts the performance of the proposed scheme based on various quantitative matrices. The quantitative analysis is categorized into two parts. The parameter such as Pearson correlation coefficient (PCC), universal image quality index (IQI), structural similarity index measurement (SSIM), and contrast improvement index (CII) is used to evaluate the quality of the enhanced image. However, error estimation is done using average mean brightness error (AMBE) and mean absolute

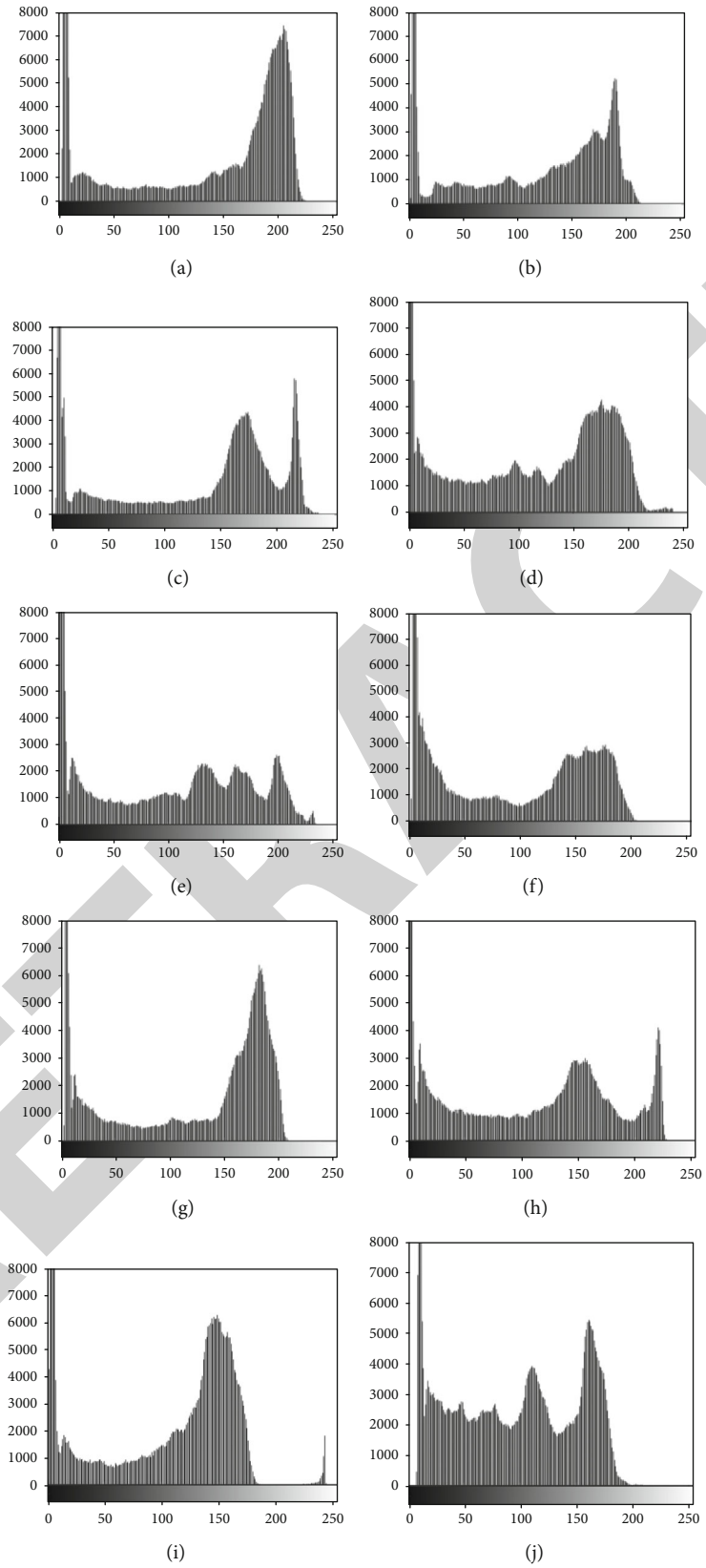

Figure 6: Histograms corresponding to original mammogram images (I-1 to I-10).

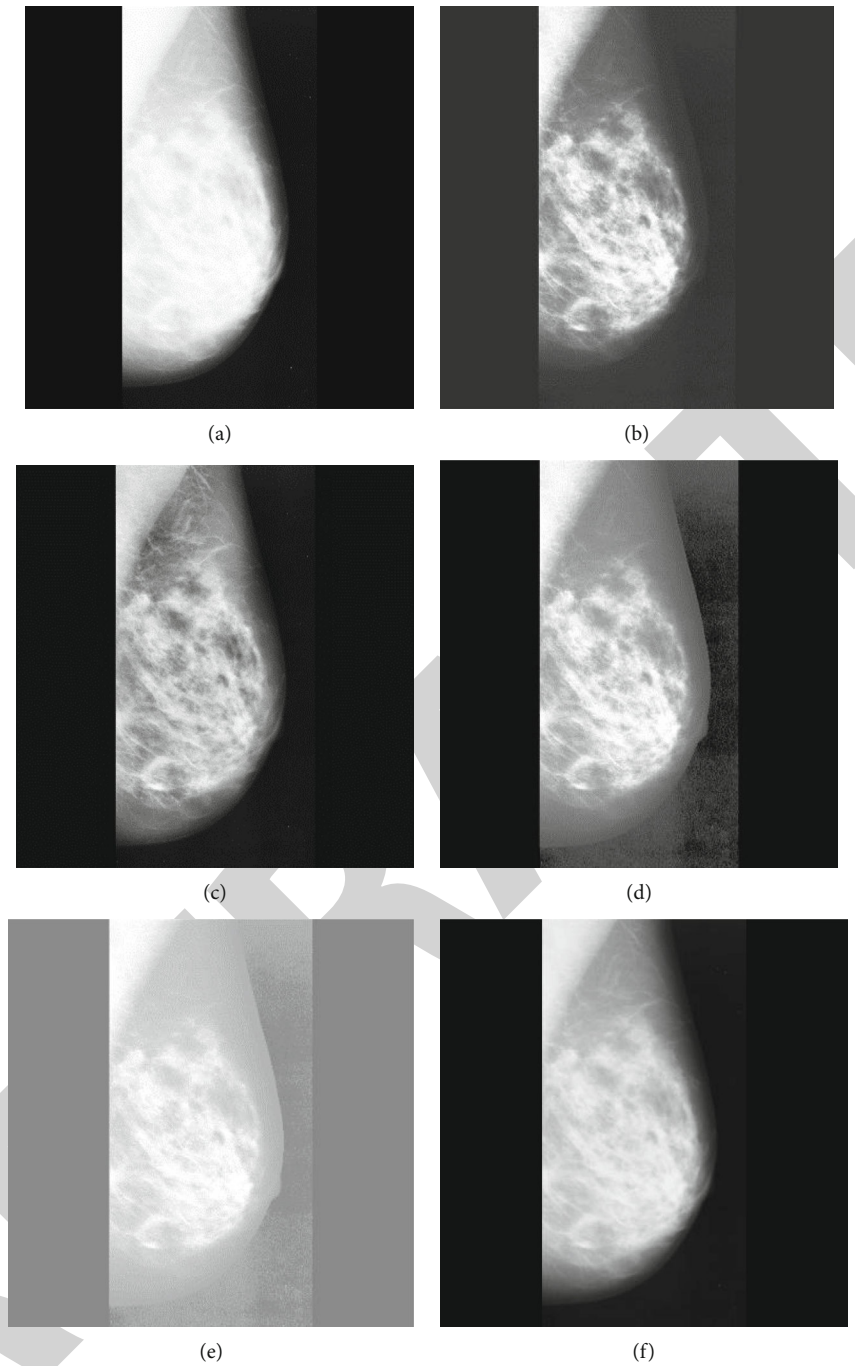

Figure 7: Enhanced image I-1 (a) using AGCWD, (b) using BBHE, (c) using CLAHE, (d) using DSIHE, (e) using HE, and (f) using proposed method.

error (MAE). The brief of all the evaluation matrices is given under.

The PCC is used to check the degree of correlation between two samples of equal size [41]. Equation (8) is used to calculate the PCC between the original image x and the enhanced image y, of dimension (m, n).

$$\mathrm{PCC} = \frac{\sum_{i=1}^{m}\sum_{j=1}^{n}((x(i,j)-\bar{x})(y(i,j)-\bar{y}))}{\sqrt{\sum_{i=1}^{m}\sum_{j=1}^{n}((x(i,j)-\bar{x})^2}\sqrt{\sum_{i=1}^{m}\sum_{j=1}^{n}((y(i,j)-\bar{y})^2}}, \quad (8)$$

where $\bar{x}$ and $\bar{y}$ denote the mean of sample x and sample y, respectively. The PCC values are ranging from 0 to 1 where 0 reflects no correlation and 1 indicates high correlation between the original and the corresponding enhanced image.

Universal image quality index (IQI) is used to check the distortion of the images as a combination of three factors: loss of correlation, luminance distortion, and contrast distortion [42]. The dynamic range of IQI is [-1,1]. The mathematical expression of IQI is given as follows.

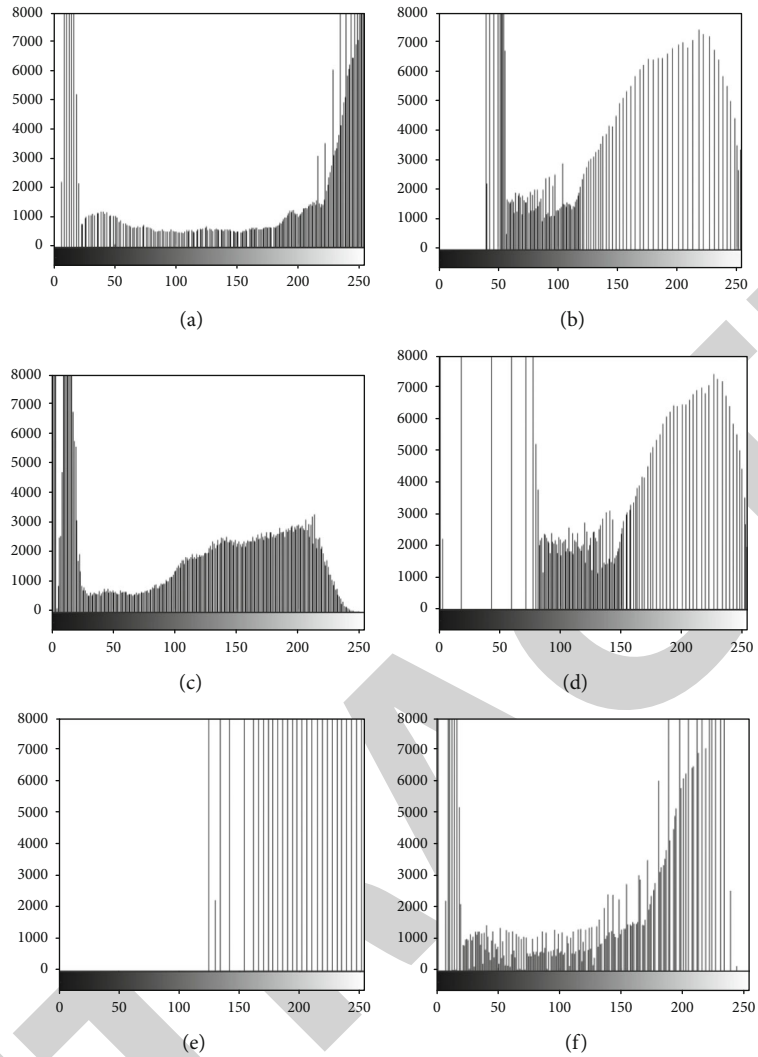

Figure 8: Histogram corresponding to enhanced mammogram image I-1 (a) using AGCWD, (b) using BBHE, (c) using CLAHE, (d) using DSIHE, (e) using HE, and (f) using the proposed method.

Table 1: Comparison using PCC, IQI, SSIM, CII, AMBE, and MAE parameter.

Image	PCC	IQI	SSIM	CII	AMBE	MAE
I-1	0.9978	0.9128	0.9113	1.1087	15.4932	15.4932
I-2	0.9976	0.9163	0.9152	1.0625	14.1323	14.1323
I-3	0.9965	0.9226	0.9215	1.0669	12.8455	12.8455
I-4	0.9962	0.9146	0.9131	1.0581	18.2951	18.2959
I-5	0.9939	0.9101	0.9089	1.0851	14.1178	14.1178
I-6	0.9967	0.9147	0.9132	1.1751	15.6748	15.6749
I-7	0.9983	0.9358	0.9347	1.1644	15.7191	15.7191
I-8	0.9924	0.9140	0.9128	1.1087	14.5033	14.5033
I-9	0.9967	0.9038	0.9025	1.0451	20.2628	20.2630
I-10	0.9970	0.9080	0.9061	1.1860	25.0460	25.0460
Average	**0.9963**	**0.9153**	**0.9139**	**1.1061**	**16.6090**	**16.6091**

$$x_0 = \{x_i | i = 1, 2, \cdots, N\}, \tag{9}$$

$$x_t = \{x_{t_i} | i = 1, 2, \cdots, N\}, \tag{10}$$

$$\text{IQI} = \frac{\sigma_{x_0 x_t}}{\sigma_{x_0}\sigma_{x_t}} \cdot \frac{2\bar{x}_0\bar{x}_t}{\bar{x}_0^2 + \bar{x}_t^2} \bullet \frac{2\sigma_{x_0}\sigma_{x_t}}{\sigma_{x_0}^2 + \sigma_{x_t}^2}. \tag{11}$$

The enhanced image quality can be measured by comparing the structural similarity index measurement (SSIM) between the original image and its enhanced version [43]. It is composed of three subparts—luminance term L, contrast term C, and the Structural term S. Here, x denotes the input image, and y denotes the corresponding enhanced image. SSIM can be calculated as

$$\text{SSIM}\,(x, y) = L * C * S. \tag{12}$$

Expanding the eq. (12), the following equation of SSIM is observed.

$$\text{SSIM}(x, y) = \left[\{L(x, y)^{\alpha}\} \bullet \left\{C(x, y)^{\beta}\right\} \bullet \{S(x, y)^{\gamma}\}\right], \tag{13}$$

where $\alpha > 0$, $\beta > 0$, and $\gamma > 0$ are parameters used to adjust the three component's relative importance. SSIM depends upon the luminosity, contrast, and structural disorders, which plays a crucial role in image enhancement. The luminance $L\,(x, y)$, contrast $C\,(x, y)$, and structural terms $S\,(x, y)$ can be expressed as

$$\begin{aligned} L(x, y) &= \frac{\left(2\mu_x\mu_y + C_1\right)}{\left(\mu_x^2 + \mu_y^2 + C_1\right)}, \\ C(x, y) &= \frac{\left(2\sigma_x\sigma_y + C_2\right)}{\left(\sigma_x^2 + \sigma_y^2 + C_2\right)}, \\ S(x, y) &= \frac{\left(\sigma_{xy} + C_3\right)}{\left(\sigma_x + \sigma_y + C_3\right)}, \end{aligned} \tag{14}$$

where μ_x, $\mu_{y,}\sigma_x, \sigma_y$, and σ_{xy} are the local means, standard deviations, and cross-covariance for images x, y. Now, the modified SSIM can be expressed as

$$\text{SSIM} = \frac{\left(2\mu_x\mu_y + C_1\right)\left(2\sigma_x\sigma_y + C_2\right)\left(\sigma_{xy} + C_3\right)}{\left(\mu_x^2 + \mu_y^2 + C_1\right)\left(\sigma_x^2 + \sigma_y^2 + C_2\right)}. \tag{15}$$

The higher SSIM values produce better performance in terms of image quality [28, 44]. The contrast enhancement can be evaluated using the contrast improvement index (CII), which is one of the most well-known image enhancement measures as expressed as

$$\text{CII} = \frac{C_{pro}}{C_{org}}. \tag{16}$$

C_{org} stands for the local contrast's average intensity in the original image, while C_{pro} stands for the local contrast's average intensity in the output image. CII helps to analyze the improvement in the contrast of the enhanced image with respect to the original image. The higher score of CII indicates that the processed image quality is better [22].

The information loss is evaluated using two error estimating parameters called average mean brightness error (AMBE) and mean absolute error (MAE). AMBE plays a significant role in defining the absolute value of error between the enhanced and the original image. AMBE can be judged in order to know the information losses, and it is desirable to have as low AMBE as possible while enhancement [41, 45–47]. AMBE is related to the deviations during the brightness of the enhanced image compared to the original image. AMBE can be calculated as follows:

$$\text{AMBE} = \left|E\left[I'\right] - E[I]\right|, \tag{17}$$

where $E\,[I']$ and $E\,[I]$ refer to the mean gray levels of the enhanced and the original image, respectively. Equation (19) is used to calculate $E\,[I']$ and $E\,[I]$ for both I and I' is the images of size (m, n).

$$E[I] = \frac{1}{mn}\sum_{x=1}^{m}\sum_{y=1}^{n} I(x, y), \tag{18}$$

$$E\left[I'\right] = \frac{1}{mn}\sum_{x=1}^{m}\sum_{y=1}^{n} I'(x, y). \tag{19}$$

MAE is related to finding the performance error in the enhancement. So, it is desired to have a low MAE while designing any enhancement methodology. It helps to evaluate the error per pixel, and so the lesser MAE is desired for the least distorted image. MAE can be calculated as [48]

$$\text{MAE} = \frac{1}{mn}\sum_{i=1}^{m}\sum_{j=1}^{n}\left|I'(i, j) - I(i, j)\right|, \tag{20}$$

where I and I' refer to the original and the enhanced image, respectively, and both are of size (m, n).

The simulation results of the proposed scheme using all such performance metrics over the ten sample images are discussed here. Table 1 shows the outcome of the proposed scheme using these metrics, and the observed value meets the objectives satisfactorily. The average result of all the images is given in bold letters and also fulfills the requirements.

Tables 2–7 and Figures 9–14 show the comparative analysis of the proposed scheme with other traditional methods such as HE and CLAHE. Using the selected image database, all the traditional methods are also implemented in MATLAB for comparison with the proposed scheme. Table 2 represents the comparative analysis of the proposed scheme with other traditional methods using the PCC parameter. In this comparison, one can observe the proposed

Table 2: Comparison using PCC parameter.

Image	HE	CLAHE	BBHE	DSIHE	Proposed method
I-1	0.9650	0.9857	0.9453	0.9638	**0.9978**
I-2	0.9746	0.9853	0.9697	0.9678	**0.9976**
I-3	0.9764	0.9906	0.9573	0.9736	**0.9965**
I-4	0.9862	0.9644	0.9718	0.9820	**0.9962**
I-5	0.9705	0.9742	0.9838	0.9689	**0.9939**
I-6	0.9684	0.9690	0.9758	0.9681	**0.9967**
I-7	0.9767	0.9822	0.9474	0.9748	**0.9983**
I-8	0.9839	0.9759	0.9828	0.9784	**0.9924**
I-9	0.9761	0.9808	0.9524	0.9714	**0.9967**
I-10	**0.9977**	0.9589	0.9786	**0.9983**	**0.9970**
Average	0.9776	0.9767	0.9665	0.9747	**0.9963**

Table 3: Comparison using IQI parameter.

Image	HE	CLAHE	BBHE	DSIHE	Proposed method
I-1	0.2243	0.3135	0.2316	0.2408	**0.9128**
I-2	0.1522	0.2422	0.2377	0.8154	**0.9163**
I-3	0.1676	0.2452	0.2137	0.8113	**0.9226**
I-4	0.2338	0.2943	0.3062	0.8168	**0.9146**
I-5	0.1193	0.2327	0.2469	0.8358	**0.9101**
I-6	0.1398	0.2330	0.2375	0.8230	**0.9147**
I-7	0.1789	0.2423	0.1958	0.8095	**0.9358**
I-8	0.1339	0.2361	0.2407	0.8466	**0.9140**
I-9	0.2326	0.3033	0.2579	0.7559	**0.9038**
I-10	0.2644	0.3096	0.3600	0.3975	**0.9080**
Average	0.1847	0.2652	0.2528	**0.7153**	**0.9153**

Table 4: Comparison using SSIM parameter.

Image	HE	CLAHE	BBHE	DSIHE	Proposed method
I-1	0.2130	0.3115	0.2282	0.2382	**0.9113**
I-2	0.1442	0.2398	0.2345	0.8142	**0.9152**
I-3	0.1580	0.2424	0.2110	0.8101	**0.9215**
I-4	0.2192	0.2945	0.3014	0.8152	**0.9131**
I-5	0.1099	0.2304	0.2425	0.8339	**0.9089**
I-6	0.1313	0.2309	0.2329	0.8216	**0.9132**
I-7	0.1688	0.2399	0.1927	0.8086	**0.9347**
I-8	0.1236	0.2334	0.2365	0.8445	**0.9128**
I-9	0.2227	0.3011	0.2540	0.7555	**0.9025**
I-10	0.2474	0.3069	0.3539	0.3926	**0.9061**
Average	0.1738	0.2631	0.2488	**0.7135**	**0.9139**

Table 5: Comparison Using CII parameter.

Image	HE	CLAHE	BBHE	DSIHE	Proposed method
I-1	0.5652	1.0783	0.9348	1.1000	**1.1087**
I-2	0.4208	1.0542	0.9375	**1.0625**	**1.0625**
I-3	0.4226	1.0126	0.9205	**1.0669**	**1.0669**
I-4	0.5187	1.0249	0.9046	**1.0581**	**1.0581**
I-5	0.4298	1.0681	0.9660	**1.0851**	**1.0851**
I-6	0.4654	1.1198	1.0553	**1.1751**	**1.1751**
I-7	0.4612	1.0868	1.0046	**1.1644**	**1.1644**
I-8	0.4217	1.0739	0.9783	**1.1087**	**1.1087**
I-9	0.5123	1.0000	0.9098	**1.0451**	**1.0451**
I-10	0.6047	1.1581	1.0186	1.1721	**1.1860**
Average	0.4822	1.0677	0.9630	**1.1038**	**1.1061**

Table 6: Comparison using AMBE parameter.

Image	HE	AGCWD	BBHE	Proposed method
I-1	102.3144	16.0910	21.4899	**15.4932**
I-2	137.2902	14.7741	22.3837	**14.1323**
I-3	131.1784	13.1972	21.5013	**12.8455**
I-4	111.1211	19.4299	26.2448	**18.2951**
I-5	139.9295	14.3150	22.3325	**14.1178**
I-6	141.7641	16.1731	21.5008	**15.6748**
I-7	131.8405	15.9564	23.1687	**15.7191**
I-8	139.6881	14.7140	22.8224	**14.5033**
I-9	116.1674	22.6745	27.1185	**20.2628**
I-10	112.2327	25.4007	31.8028	**25.0460**
Average	126.3526	17.2726	24.0365	16.6090

Table 7: Comparison using MAE parameter.

Image	HE	AGCWD	BBHE	Proposed method
I-1	102.3144	16.0910	36.4021	**15.4932**
I-2	137.2902	14.7741	26.8607	**14.1323**
I-3	131.1784	13.1972	31.3422	**12.8455**
I-4	111.1211	19.4299	29.4851	**18.2959**
I-5	139.9295	14.3150	24.0376	**14.1178**
I-6	141.7641	16.1731	23.2831	**15.6749**
I-7	131.8405	15.9564	32.3504	**15.7191**
I-8	139.6881	14.7140	25.1304	**14.5033**
I-9	116.1674	22.6745	31.2155	**20.2630**
I-10	112.2327	25.4007	31.8028	**25.0460**
Average	126.3526	17.2726	29.1910	**16.6091**

scheme performs better in all the cases, as shown in bold letters. The average values over all the ten images are also given in this table. Here, again, the average value of the proposed scheme fulfills the required objective. In order to extend the above-given comparison, we consider all 322 mammogram images of the dataset, and the results are shown in Figure 9. It is observed from Figure 9 that the proposed method has a significantly higher average PCC value when compared with other existing methods.

The proposed scheme is also compared to other conventional approaches using the IQI parameter for ten sample images and is shown in Table 3. It can be observed from

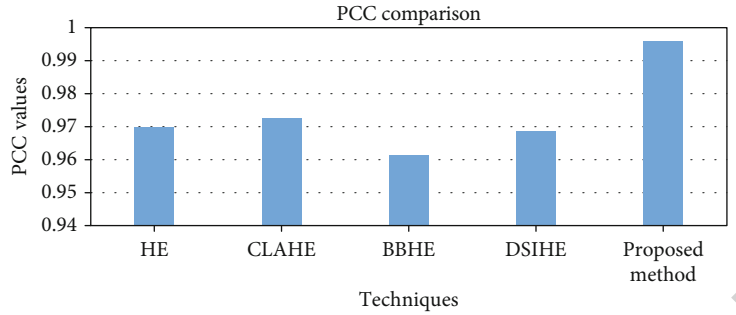

Figure 9: Graphical comparison using PCC parameter on all 322 images of mini-MIAS dataset.

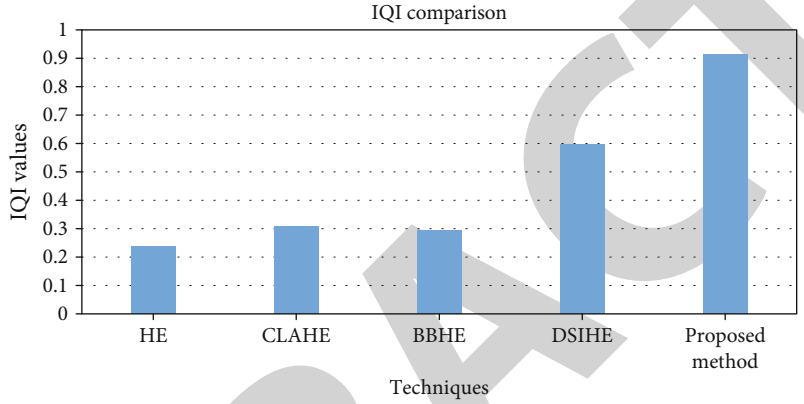

Figure 10: Graphical comparison using IQI parameter on all 322 images of mini-MIAS dataset.

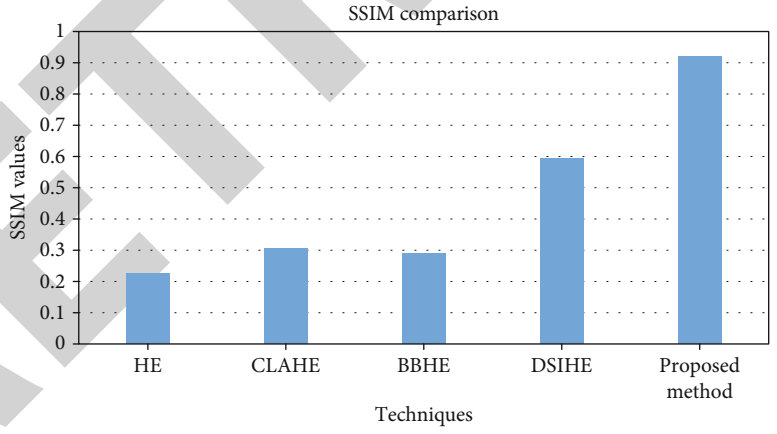

Figure 11: Graphical comparison using SSIM parameter on all 322 images of mini-MIAS dataset.

the table that the proposed scheme has better IQI values than the other traditional methods, as it produces the least distortion in the enhanced images and hence preserves its quality. It is also evident from Figure 10 that the proposed technique shows better results for average IQI values on all 322 mammogram images.

The result of the comparison between the various methods based on the SSIM parameter is given in Table 4. In this table, it is observed that the proposed method produces significantly good results as compared to other methods. The average SSIM values of ten images of the proposed method are high, which concludes high similarity between the original and enhanced image. Figure 11 shows the better performance of the proposed method for all 322 mammogram images of the dataset.

The CII value of DSIHE and the proposed method are comparatively equal except for two images I-1 and I-10. The results of CII are presented in Table 5. The higher CII value indicates that the enhanced image quality is better than the original image. It signifies that the proposed

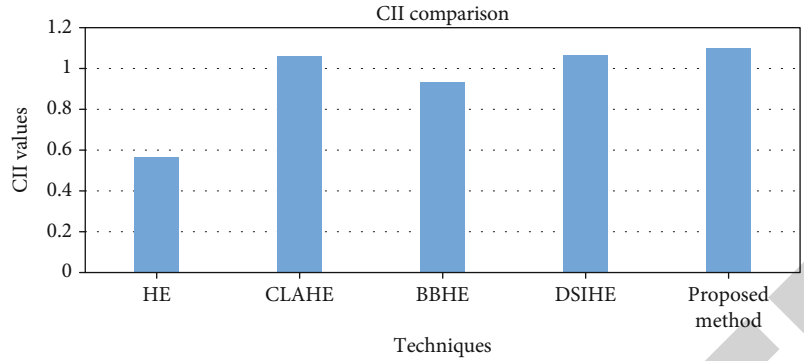

Figure 12: Graphical comparison using CII parameter on all 322 images of mini-MIAS dataset.

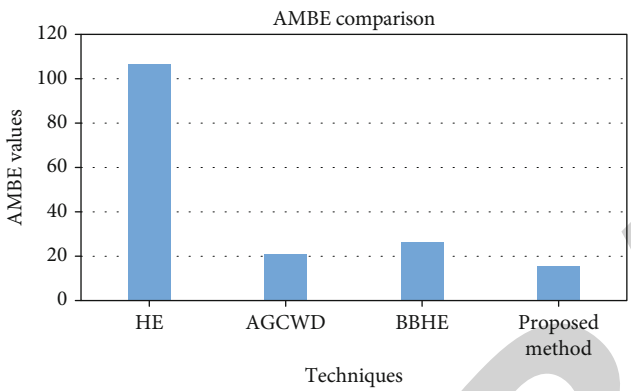

Figure 13: Graphical comparison using AMBE parameter on all 322 images of mini-MIAS dataset.

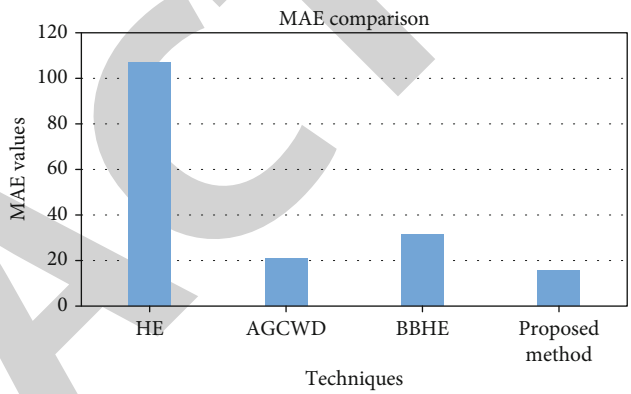

Figure 14: Graphical comparison using MAE parameter on all 322 images of mini-MIAS dataset.

technique gains better results than the existing methods. From Figure 12, it is noticed that the average CII value of the proposed method is slightly higher than other methods when tested on all 322 images.

AMBE result is analyzed for various methods in Table 6. In this, the proposed method obtains the lowest AMBE value in all the cases, which indicates better enhancement by preserving the brightness of the enhanced image compared to the original image. The average AMBE value of other methods is higher than the proposed technique, which shows good performance. The comparative results of proposed and existing methods on all 322 mammograms are graphically represented in Figure 13, which indicates that the proposed method preserves the information of the original image.

MAE parameter shows the higher performance of the proposed scheme when compared to other existing approaches, and the result is tabulated in Table 7. The comparative analysis of the proposed method with other existing methods based on MAE values on all 322 digital mammograms is shown in Figure 14. The proposed scheme gains the required low average MAE value resulting in the least distortion in the enhanced image.

The proposed method achieves the highest average value of the PCC, IQI, SSIM, and CII parameters and the lowest average value of the AMBE and MAE parameters, which showed that the resultant enhanced image contained improved image features. Therefore, in view of qualitative and quantitative assessment, it is concluded that the proposed technique obtains superior performance as compared to the other traditional methods.

In order to compare the performance of the proposed method with the state-of-art methods, we evaluated the PCC, IQI, SSIM, CII, AMBE, and MAE parameters on all 322 mammograms of the mini-MIAS dataset, and results are listed in Table 8. From Table 8, it is noticed that the proposed method obtains the higher average values of PCC, IQI, SSIM, and CII parameters and lower average values of AMBE and MAE parameters. The PCC value for FWHE is the lowest one with an average of 0.908, whereas the proposed method achieves the highest value with an average of 0.996, which indicates the high correlation of the enhanced image with the original image. Furthermore, the proposed method achieves the highest average value of 0.913 and 0.921 for IQI and SSIM parameters, whereas RMSHE has the lowest value of 0.686 for IQI parameter, and FWHE has the lowest value of 0.681 for SSIM parameter, respectively. It shows that the proposed method achieves better quality and preserves mammogram images' structure. FC-CLAHE obtains the highest value of the CII parameter with an average of 2.983, whereas our proposed method achieves the second-highest value with an average of 1.098, but it still provides sufficient contrast improvement of the

Table 8: Comparison of state-of-art methods and proposed method on 322 digital mammograms of mini-MIAS dataset.

Enhancement methods	Performance measures					
	PCC	IQI	SSIM	CII	AMBE	MAE
RMSHE	0.913	0.686	0.783	0.928	24.017	34.237
DWT-SVD	0.925	0.864	0.786	0.962	29.568	32.314
FC-CLAHE	0.934	0.713	0.716	2.983	12.207	28.303
FWHE	0.908	0.749	0.681	1.007	12.563	25.128
Proposed method	0.996	0.912	0.921	1.098	15.732	15.624

mammogram images. DWT-SVD scores the highest value of the AMBE parameter with an average of 29.568, while FC-CLAHE scores the lowest value with an average of 12.207. The proposed method attains an average AMBE score of 15.732, which is optimum and able to preserve the naturalness of the mammogram image. It is also observed from Table 8 that the MAE parameter average value is 15.624 for the proposed method, which is the lowest among other state-of-art methods. This signifies that the proposed method attains the significant contrast-enhanced images that show the least distortion after enhancement. It is concluded from the above discussion that our proposed method obtained the best value on PCC, IQI, and SSIM parameters and second best, optimal and lowest value on CII, AMBE, and MAE parameters, respectively, resulting in significantly improved contrast-enhanced mammogram images.

From the above discussion, it is observed that the proposed method performs significantly better as compared to other traditional methods like HE, CLAHE, BBHE, and DSHIE when tested with PCC, IQI, SSIM, CII, AMBE, and MAE parameters. In order to prove the suitability of this method in the contemporary scenario, we also evaluated our technique on PCC, IQI, SSIM, CII, AMBE, and MAE parameters and compared with other state-of-art methods and find out that the proposed method performs well for some parameters by achieving best values, but the value of some parameters is slightly down but still optimum. Hence, it is concluded that the proposed method's overall performance is better compared to the state-of-art methods.

5. Conclusion

This paper proposes a new technique for enhancing mammogram images based on luminosity and contrast enhancement. First, the mammogram image's luminosity is controlled using the CAGC approach, and then, the processed image is undergone for contrast enhancement using the combined operation of DWT-SVD. The adaptive gamma correction dynamically calculates the intensity transformation function according to mammogram statistical characteristics. Further, sufficient contrast enhancement of mammograms is achieved using the DWT-SVD method on gamma-corrected images. This method preserves the edge details by applying SVD only on the *LL* subband obtained using DWT. The experimental results clearly help to distinguish the proposed method better than the other prevailing methods and state-of-art methods. Within the framework of mammogram enhancement, the proposed approach also ensures a balance between maintaining image quality after enhancement and minimizing image enhancement errors. The observed outcome of the proposed scheme can be helpful to the medical practitioners in the identification of the cancerous locations during the screening of mammogram images.

Although this research performs well on the qualitative and quantitative assessment, still some issues remain to be solved. Till now, we have not evaluated the performance of our proposed method in the presence of noise. The clinical evaluation of the proposed method on mammogram images is not performed yet. In future, we evaluate the performance of our proposed method in various noisy environments with clinical trials.

Data Availability

Data and results are available on request from the corresponding author.

Conflicts of Interest

The authors declare that they have no conflicts of interest.

References

[1] L. M. Wun, R. M. Merrill, and E. J. Feuer, "Estimating lifetime and age-conditional probabilities of developing cancer," *Lifetime Data Analysis*, vol. 4, no. 2, pp. 169–186, 1998.

[2] R. Mousa, Q. Munib, and A. Moussa, "Breast cancer diagnosis system based on wavelet analysis and fuzzy-neural," *Expert Systems with Applications*, vol. 28, no. 4, pp. 713–723, 2005.

[3] X. Gao, Y. Wang, X. Li, and D. Tao, "On combining morphological component analysis and concentric morphology model for mammographic mass detection," *IEEE Transactions on Information Technology in Biomedicine*, vol. 14, no. 2, pp. 266–273, 2010.

[4] Z. Rahman, P. Yi-Fei, M. Aamir, S. Wali, and Y. Guan, "Efficient image enhancement model for correcting uneven illumination images," *IEEE Access*, vol. 8, pp. 109038–109053, 2020.

[5] Z. Rahman, M. Aamir, Y. F. Pu, F. Ullah, and Q. Dai, "A smart system for low-light image enhancement with color constancy and detail manipulation in complex light environments," *Symmetry (Basel)*, vol. 10, no. 12, p. 718, 2018.

[6] A. Khmag, A. R. Ramli, and N. Kamarudin, "Clustering-based natural image denoising using dictionary learning approach in wavelet domain," *Soft Computing*, vol. 23, no. 17, pp. 8013–8027, 2019.

[7] A. Khmag, "Digital image noise removal based on collaborative filtering approach and singular value decomposition," *Multimedia Tools and Applications*, vol. 81, no. 12, pp. 16645–16660, 2022.

[8] M. J. Shensa, "The discrete wavelet transform: wedding the a trous and Mallat algorithms," *IEEE Transactions on Signal Processing*, vol. 40, no. 10, pp. 2464–2482, 1992.

[9] V. C. Klema and A. J. Laub, "The singular value decomposition: its computation and some applications," *IEEE Transactions on Automatic Control*, vol. 25, no. 2, pp. 164–176, 1980.

[10] P. S. J.-D. Mammo, "Undefined the mammographic image analysis society digital mammogram database," 1994, https://cir.nii.ac.jp/.

[11] N. Patrick, H. P. Chan, B. Sahiner, and D. Wei, "An adaptive density-weighted contrast enhancement filter for mammographic breast mass detection," *IEEE Transactions on Medical Imaging*, vol. 15, no. 1, pp. 59–67, 1996.

[12] E. D. Pisano, S. Zong, B. M. Hemminger et al., "Contrast limited adaptive histogram equalization image processing to improve the detection of simulated spiculations in dense mammograms," *Journal of Digital Imaging*, vol. 11, no. 4, pp. 193–200, 1998.

[13] Y. Jin, L. M. Fayad, and A. F. Laine, "Contrast enhancement by multiscale adaptive histogram equalization," in *Wavelets: Applications in Signal and Image Processing IX*, vol. 4478, pp. 206–213, San Diego, CA, United States, 2001.

[14] Z. Wu, J. Yuan, B. Lv, and X. Zheng, "Digital mammography image enhancement using improved unsharp masking approach," in *Proc -2010 3rd Int Congr image signal process CISP 2010*, vol. 2, pp. 668–672, Yantai, China, 2010.

[15] M. Sundaram, K. Ramar, N. Arumugam, and G. Prabin, "Histogram based contrast enhancement for mammogram images," in *2011 International conference on signal processing, communication, computing and networking technologies*, pp. 842–846, Thuckalay, India, 2011.

[16] M. Sundaram, K. Ramar, N. Arumugam, and G. Prabin, "Histogram modified local contrast enhancement for mammogram images," *Applied Soft Computing*, vol. 11, no. 8, pp. 5809–5816, 2011.

[17] K. Panetta, Y. Zhou, S. Agaian, and H. Jia, "Nonlinear unsharp masking for mammogram enhancement," *IEEE Transactions on Information Technology in Biomedicine*, vol. 15, no. 6, pp. 918–928, 2011.

[18] S. C. Huang, F. C. Cheng, and Y. S. Chiu, "Efficient contrast enhancement using adaptive gamma correction with weighting distribution," *IEEE Transactions on Image Processing*, vol. 22, no. 3, pp. 1032–1041, 2013.

[19] M. Kim and M. G. Chung, "Recursively separated and weighted histogram equalization for brightness preservation and contrast enhancement," *IEEE Transactions on Consumer Electronics*, vol. 54, no. 3, pp. 1389–1397, 2008.

[20] A. Kaur and M. Singh, "Image enhancement using recursive adaptive gamma correction," *International Journal of Innovations in Engineering and Technology (IJIET)*, vol. 4, pp. 1–9, 2014.

[21] S. Anand and S. Gayathri, "Mammogram image enhancement by two-stage adaptive histogram equalization," *Optik (Stuttg)*, vol. 126, no. 21, pp. 3150–3152, 2015.

[22] S. Jenifer, S. Parasuraman, and A. Kadirvelu, "Contrast enhancement and brightness preserving of digital mammograms using fuzzy clipped contrast-limited adaptive histogram equalization algorithm," *Applied Soft Computing*, vol. 42, pp. 167–177, 2016.

[23] Y. T. Kim, "Contrast enhancement using brightness preserving bi-histogram equalization," *IEEE Transactions on Consumer Electronics*, vol. 43, no. 1, pp. 1–8, 1997.

[24] Z. Yao, Z. Lai, and C. Wang, "Image enhancement based on equal area dualistic sub-image and non-parametric modified histogram equalization method," in *2016 9th International Symposium on Computational Intelligence and Design (ISCID)*, vol. 1, pp. 447–450, Hangzhou, China, 2016.

[25] K. U. Sheba and S. Gladston Raj, "Adaptive fuzzy logic based bi-histogram equalization for contrast enhancement of mammograms," in *2017 International Conference on Intelligent Computing, Instrumentation and Control Technologies (ICICICT)*, pp. 156–161, Kerala, India, 2018.

[26] C. S. Der and A. R. Ramli, "Contrast enhancement using recursive mean-separate histogram equalization for scalable brightness preservation," *IEEE Transactions on Consumer Electronics*, vol. 49, no. 4, pp. 1301–1309, 2003.

[27] H. Demirel, C. Ozcinar, and G. Anbarjafari, "Satellite image contrast enhancement using discrete wavelet transform and singular value decomposition," *IEEE Geoscience and Remote Sensing Letters*, vol. 7, no. 2, pp. 333–337, 2010.

[28] F. Kallel and A. Ben Hamida, "A new adaptive gamma correction based algorithm using DWT-SVD for non-contrast CT image enhancement," *IEEE Transactions on Nanobioscience*, vol. 16, no. 8, pp. 666–675, 2017.

[29] M. Zhou, K. Jin, S. Wang, J. Ye, and D. Qian, "Color retinal image enhancement based on luminosity and contrast adjustment," *IEEE Transactions on Biomedical Engineering*, vol. 65, no. 3, pp. 521–527, 2018.

[30] B. Gupta and M. Tiwari, "Color retinal image enhancement using luminosity and quantile based contrast enhancement," *Multidimensional Systems and Signal Processing*, vol. 30, no. 4, pp. 1829–1837, 2019.

[31] G. Palanisamy, P. Ponnusamy, and V. P. Gopi, "An improved luminosity and contrast enhancement framework for feature preservation in color fundus images," *Signal, Image Video Process*, vol. 13, no. 4, pp. 719–726, 2019.

[32] M. Pawar and S. Talbar, "Local entropy maximization based image fusion for contrast enhancement of mammogram," *Journal of King Saud University-Computer and Information Sciences*, vol. 33, no. 2, pp. 150–160, 2021.

[33] A. Gandhamal, S. Talbar, S. Gajre, A. F. M. Hani, and D. Kumar, "Local gray level S-curve transformation - a generalized contrast enhancement technique for medical images," *Computers in Biology and Medicine*, vol. 83, pp. 120–133, 2017.

[34] H. El Malali, A. Assir, V. Bhateja, A. Mouhsen, and M. Harmouchi, "A contrast enhancement model for X-ray mammograms using modified local s-curve transformation based on multi-objective optimization," *IEEE Sensors Journal*, vol. 21, no. 10, pp. 11543–11554, 2021.

[35] V. Magudeeswaran and K. Balasubramanian, "Fuzzy weighted histogram equalisation for contrast enhancement of mammogram images," *International Journal of Biomedical Engineering and Technology*, vol. 28, no. 3, pp. 232–242, 2018.

[36] A. A. Siddiqi, A. Khawaja, and A. Hashmi, "A novel fuzzy blend scheme for image enhancement of CT scans bearing liver cancer," *Computer Methods in Biomechanics and Biomedical Engineering: Imaging & Visualization*, vol. 9, no. 6, pp. 581–586, 2021.

[37] A. K. Bhandari, A. Kumar, G. K. Singh, and V. Soni, "Dark satellite image enhancement using knee transfer function and gamma correction based on DWT–SVD," *Multidimensional Systems and Signal Processing*, vol. 27, no. 2, pp. 453–476, 2016.

[38] A. V. Archana, "A survey on image contrast enhancement using genetic algorithm," *International Journal of Scientific and Research Publications*, vol. 2, no. 7, 2012.

[39] G. S. Archana, A. Verma, and N. Kumar, "Gray level enhancement to emphasize less dynamic region within image using genetic algorithm," in *2013 3rd IEEE International Advance Computing Conference (IACC)*, pp. 1171–1176, Ghaziabad, India, 2013.

[40] R. C. Gonzalez and R. E. Woods, *Digital Image Processing*, Pearson, 2018.

[41] S. Z. Ramadan, "Methods used in computer-aided diagnosis for breast cancer detection using mammograms: a review," *Journal of Healthcare Engineering*, vol. 2020, Article ID 9162464, 21 pages, 2020.

[42] Z. Wang and A. C. Bovik, "A universal image quality index," *IEEE Signal Processing Letters*, vol. 9, no. 3, pp. 81–84, 2002.

[43] Z. Wang, A. C. Bovik, H. R. Sheikh, and E. P. Simoncelli, "Image quality assessment: from error visibility to structural similarity," *IEEE Transactions on Image Processing*, vol. 13, no. 4, pp. 600–612, 2004.

[44] P. Kandhway, A. K. Bhandari, and A. Singh, "A novel reformed histogram equalization based medical image contrast enhancement using krill herd optimization," *Biomedical Signal Processing and Control*, vol. 56, article 101677, 2020.

[45] M. Hazarika and L. B. Mahanta, "A new breast border extraction and contrast enhancement technique with digital mammogram images for improved detection of breast cancer," *Asian Pacific Journal of Cancer Prevention: APJCP*, vol. 19, no. 8, pp. 2141–2148, 2018.

[46] Z. Huang, Z. Wang, J. Zhang, Q. Li, and Y. Shi, "Image enhancement with the preservation of brightness and structures by employing contrast limited dynamic quadri-histogram equalization," *Optik*, vol. 226, Part 1, article 165877, 2021.

[47] A. Wadhwa and A. Bhardwaj, "Enhancement of MRI images of brain tumor using Grünwald Letnikov fractional differential mask," *Multimedia Tools and Applications*, vol. 79, no. 35-36, pp. 25379–25402, 2020.

[48] J. Kirubakaran, G. K. D. P. Venkatesan, K. Sampath Kumar, M. Kumaresan, and S. Annamalai, "Echo state learned compositional pattern neural networks for the early diagnosis of cancer on the internet of medical things platform," *Journal of Ambient Intelligence and Humanized Computing*, vol. 12, no. 3, pp. 3303–3316, 2021.